SUPPLEMENTARY MATERIAL

High density lipoprotein mediates anti-inflammatory transcriptional reprogramming of macrophages via the transcriptional repressor ATF3

Dominic De Nardo[1]*, Larisa I. Labzin[1]*, Hajime Kono[2], Reiko Seki[2], Susanne V. Schmidt[3], Marc Beyer[3], Dakang Xu[4,5], Sebastian Zimmer[6], Catharina Lahrmann[6], Frank A. Schildberg[7], Johanna Vogelhuber[1], Michael Kraut[3], Thomas Ulas[3], Anja Kerksiek[8], Wolfgang Krebs[3], Niklas Bode[6], Alena Grebe[1], Michael L. Fitzgerald[9], Nicholas J. Hernandez[9], Bryan Williams[4], Percy Knolle[7], Manfred Kneilling[10,11], Martin Röcken[10], Dieter Lütjohann[8], Samuel D. Wright[12], Joachim L. Schultze[3]* and Eicke Latz[1,13,14]*

[1]Institute of Innate Immunity, University Hospitals, Biomedical Centre, University of Bonn, Germany. [2]Department of Internal Medicine, Teikyo University School of Medicine, Tokyo, Japan. [3]Life and Medical Sciences Institute (LIMES), University of Bonn, Germany. [4]Monash Institute of Medical Research, Monash University, Melbourne, Victoria, Australia. [5]Institute of Ageing Research, Hangzhou Normal University School of Medicine, Hangzhou, China. [6]Department of Medicine/Cardiology, University of Bonn, Germany. [7]Institutes of Molecular Medicine and Experimental Immunology, University of Bonn, Germany. [8]Instititute for Clinical Chemistry and Clinical Pharmacology, University of Bonn, Germany. [9]Lipid Metabolism Unit, Massachusetts General Hospital, Harvard Medical School, Boston, USA. [10]Department of Dermatology and [11]Werner Siemens Imaging Center, Department of Preclinical Imaging and Radiopharmacy Eberhard Karls University, Tuebingen, Germany. [12]Cardiovascular Therapeutics, CSL Limited, Parkville, Australia. [13]Division of Infectious Diseases and Immunology, University of Massachusetts Medical School, Worcester, USA. [14]German Center for Neurodegenerative Diseases (DZNE), Bonn, Germany.

** These authors contributed equally to this work.*

Sup.Figure 1

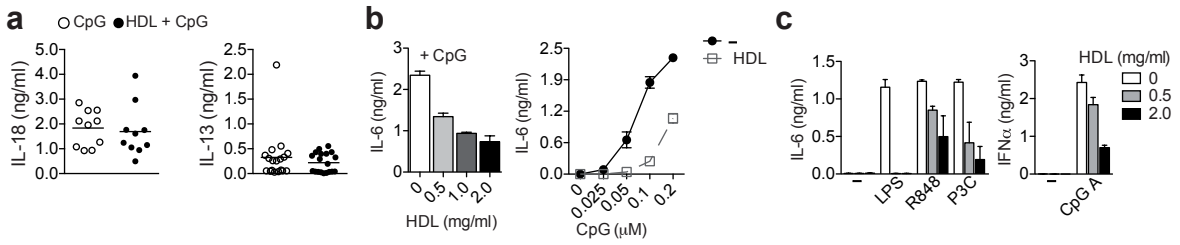

Supplementary Figure 1 Detailed characterisation of the effect of HDL on TLR-induced cytokine secretion. **a,** C57BL/6 mice were injected i.p with 2 mg recombinant HDL or PBS 6 h before subsequent injection with CpG (20 μg) and D-gal (10 mg), 1 h later serum was collected and cytokines were measured (IL-18 *n*=10 per group, IL-13 *n*=18 per group). **b** BMDMs were pre-treated with HDL (either 2 mg/ml or as indicated) for 6 h and stimulated overnight with CpG (100 nM or as indicated) and IL-6 measured in culture supernatants by ELISA. **c,** Human PBMCs were pre-treated for 6 h with HDL at indicated concentrations and stimulated overnight with LPS (2.5 ng/ml), R848 (100 ng/ml) or P3C (1 μg/ml) and IL-6 secretion measured (**c,** left), or PBMCs were stimulated with CpG 2336 (A-type) (1 μM) and IFNα production was measured by ELISA (**c,** right). **a,** Data are presented as mean values ±S.E.M. **b**, Data are presented as the mean ±S.D. and are representative of three independent experiments. **c**, Data is combined from three individual donors and shown as the mean ±S.E.M.

Sup.Figure 2

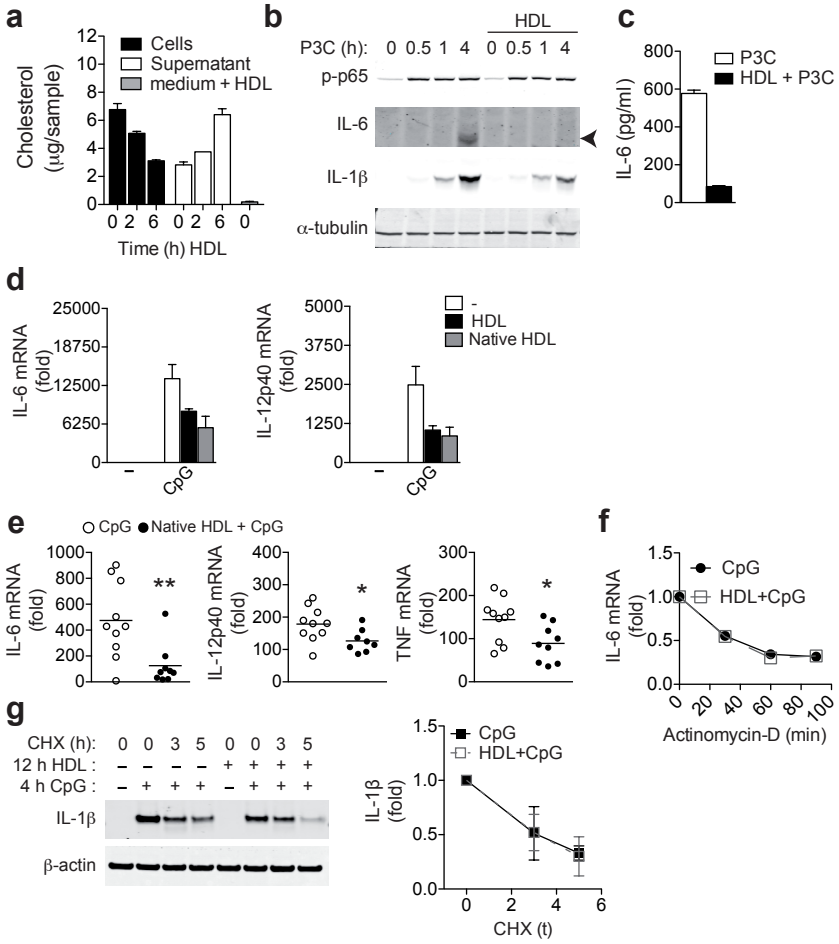

Supplementary Figure 2 HDL reduces cellular cholesterol and inhibits pro-inflammatory gene expression. **a,** Immortalised-BMDMs were treated with HDL (2 mg/ml) for indicated times and cholesterol measured by mass spectrometry from cell lysates, supernatants or media with HDL. **b,c,** Immunoblot of BMDMs pre-treated with HDL (2 mg/ml) for 6 h and stimulated for indicated times with P3C (50 ng/ml) (**b**) and ELISA of IL-6 secretion (**c**). **d,** BMDMs were pre-treated with HDL or native HDL (2 mg/ml) for 6 h and stimulated with CpG (100 nM) for 4 h before mRNA expression was measured by qPCR. **e,** C3H/HeJ mice were injected i.p with 2 mg native HDL or control filtrate 6 h before injection with CpG (20 µg) and D-gal (10 mg), 1 h later hepatic mRNA expression was measured by qPCR (CpG *n*=10, native HDL+CpG *n*=9). **f,** BMDMs were pre-treated for 6 h with HDL before 4 h with CpG (100 nM) and Actinomycin D (5 µg/ml) for the indicated times to asses the half-life of IL-6 transcripts. Data is normalised to 0 min Actinomycin D sample for respective conditions. **g**, BMDMs were pre-treated for 12 h HDL before CpG for 4 h and cyclohexamide (10 µg/ml) treatment for the indicated times to assess the half life of IL-1β protein (relative to β-actin). **a**, A representative graph of two individual experiments is presented (mean ±S.D.). **b**-**d**, A representative blot (**b**) and ELISA (mean ±S.D.) (**c**,**d**) of three individual experiments is shown. **e**, Data are presented as mean values ±S.E.M, CpG versus native HDL+CpG *p<0.05, **p<0.01. **f**, A representative graph from two independent experiments is shown. **g**, A single immunoblot is shown and densitometric analysis of IL-1β combined from three independent experiments (mean ±S.E.M).

Sup.Figure 3

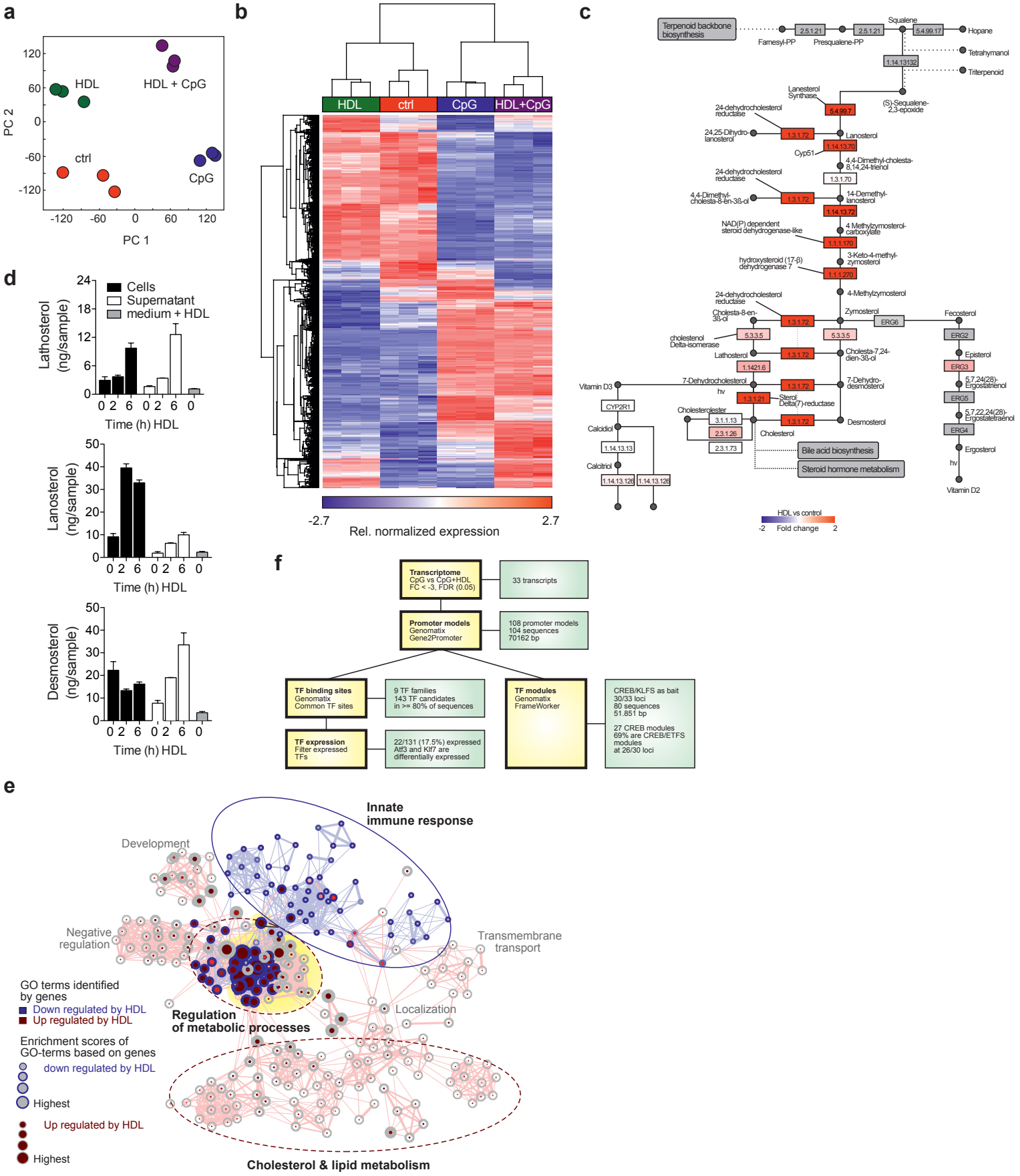
a
HDL
HDL + CpG
ctrl
CpG
PC 1
PC 2
b
HDL
ctrl
CpG
HDL+CpG
-2.7
2.7
Rel. normalized expression
c
Terpenoid backbone biosynthesis
Farnesyl-PP
Presqualene-PP
Squalene
Hopane
Tetrahymanol
Triterpenoid
Lanosterol Synthase
(S)-Sequalene-2,3-epoxide
24-dehydrocholesterol reductase
24,25-Dihydro-lanosterol
Lanosterol
Cyp51
4,4-Dimethyl-cholesta-8,14,24-trienol
14-Demethyl-lanosterol
4,4-Dimethyl-cholesta-8-en-3ß-ol
NAD(P) dependent steroid dehydrogenase-like
4 Methylzymosterol-carboxylate
hydroxysteroid (17-ß) dehydrogenase 7
3-Keto-4-methyl-zymosterol
4-Methylzymosterol
Zymosterol
Cholesta-8-en-3ß-ol
cholesterol Delta-isomerase
Cholesta-7,24-dien-3ß-ol
Fecosterol
Episterol
5,7,24(28)-Ergostatrienol
5,7,22,24(28)-Ergostatetraenol
Ergosterol
Vitamin D2
7-Dehydrocholesterol
Vitamin D3
CYP2R1
Calcidiol
Calcitriol
Sterol Delta(7)-reductase
7-Dehydro-desmosterol
Desmosterol
Cholesterolester
Cholesterol
Bile acid biosynthesis
Steroid hormone metabolism
HDL vs control
-2
Fold change
2
d
Cells
Supernatant
medium + HDL
Lathosterol (ng/sample)
Lanosterol (ng/sample)
Desmosterol (ng/sample)
Time (h) HDL
e
Innate immune response
Development
Negative regulation
Transmembrane transport
Localization
Regulation of metabolic processes
Cholesterol & lipid metabolism
GO terms identified by genes
Down regulated by HDL
Up regulated by HDL
Enrichment scores of GO-terms based on genes
down regulated by HDL
Highest
Up regulated by HDL
Highest
f
Transcriptome
CpG vs CpG+HDL
FC < -3, FDR (0.05)
33 transcripts
Promoter models
Genomatix
Gene2Promoter
108 promoter models
104 sequences
70162 bp
TF binding sites
Genomatix
Common TF sites
9 TF families
143 TF candidates
in >= 80% of sequences
TF expression
Filter expressed TFs
22/131 (17.5%) expressed
Atf3 and Klf7 are differentially expressed
TF modules
Genomatix
FrameWorker
CREB/KLFS as bait
30/33 loci
80 sequences
51.851 bp
27 CREB modules
69% are CREB/ETFS modules
at 26/30 loci

Supplementary Figure 3 Trancriptome analysis of BMDMs treated with HDL. **a**-**c**,**e**,**f**, Transcriptome data are derived from BMDMs pre-treated for 6 h with HDL (2 mg/ml) then stimulated for 4 h with CpG (100 nM). **a**, Principal component analysis of all genes demonstrating sample relationships and group associations of individual samples. **b**, Hierarchical clustering of the 1000 most variable genes within the dataset. **c** Visualisation of genes (fold change values) involved in the cholesterol biosynthesis pathway from HDL treated BMDMs. **d**, Immortalised-BMDMs were treated with 2 mg/ml HDL for indicated times and cholesterol precursors were measured by mass spectrometry. **e,** Network visualization of Gene Ontology Enrichment Analysis (GOEA) based on transcripts reduced by CpG and counter-regulated by HDL (red nodes: GO-terms, red edges: GO-term relations) or induced by CpG and counter-regulated by HDL (blue edges and nodes). **f,** Workflow scheme of transcription factor prediction modelling. **a**-**c**,**e**,**f**, At least three biological replicates per condition were generated. **d**, Representative graphs of two individual experiments are presented (mean ±S.D.).

Sup.Figure 4

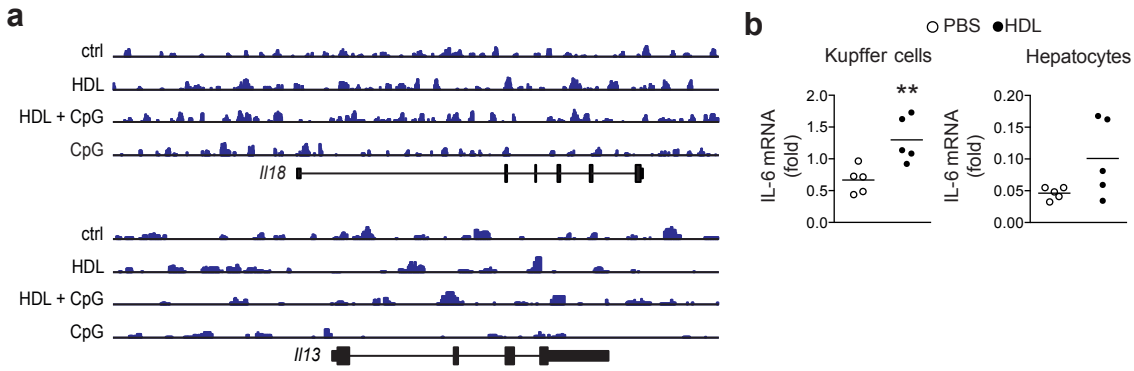

Supplementary Figure 4 ATF3 does not bind the promoters of control genes but is induced by HDL in a model of atherosclerosis. **a**, Genomic loci of *Il18* and *Il13* with ChIP-Seq signals for ATF3 binding under the various stimulation conditions. **b**, qPCR analysis of ATF3 mRNA expression in Kupffer cells or hepatocytes isolated from *Apoe*-deficient mice fed on a Western diet and injected i.v. with PBS or HDL (100 mg/kg) (*n*=5 per group)**. a**, Data was obtained from 3 biological replicates. **b**, Data are shown as the mean ±S.E.M, PBS versus HDL injected mice **p<0.01.

Sup.Figure 5

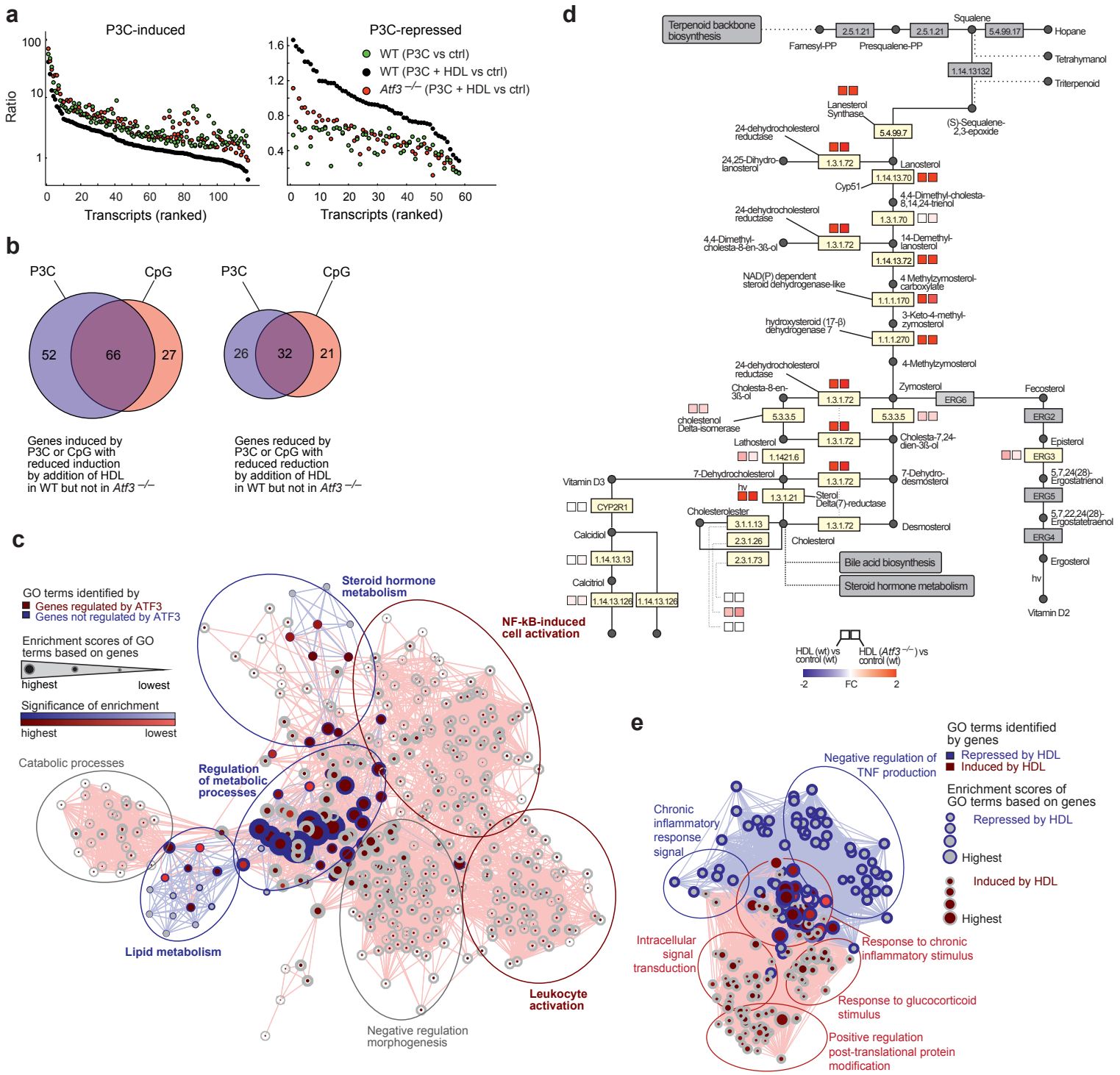

Supplementary Figure 5 Transcriptome analysis of WT vs *Atf3*-deficient BMDMs. Microarray analysis of WT or *Atf3*-deficient BMDMs pre-treated with 2 mg/ml HDL for 6 h and subsequently stimulated with CpG (100 nM) or P3C (50 ng/ml) for 4 h. **a,** Visualisation of transcripts induced or repressed by P3C in WT, counter regulated by HDL pre-treatment, and no longer modified in *Atf3*-deficient BMDMs. **b**, Venn diagrams show the overlap between CpG and P3C conditions from genes identified using the model described. **c** Network visualization of GOEA: GO-terms (nodes) and their relation (edges) based on ATF3-independent genes are shown in blue, and those based on ATF3-dependent genes are shown in red. **d**, Visualisation in fold change of genes involved in the cholesterol biosynthesis pathway from HDL treated WT or *Atf3*-deficient BMDMs. **e,** 27 of the 130 transcripts altered by CpG, counter-regulated by HDL and no longer modified in *Atf3*-deficient BMDMs are direct ATF3-target genes. Network visualization of GOEA based on transcripts reduced by CpG, counter-regulated by HDL and no longer modified in *Atf3*-deficient BMDMs showing ATF3 binding by ChIP-Seq (red nodes: GO-terms, red edges: GO-term relations) or induced by CpG and counter-regulated by HDL and no longer modified in *Atf3*-deficient BMDMs showing ATF3 binding (blue edges and nodes). **a**-**e**, At least three biological replicates per condition were generated and analysed.

Sup.Figure 6

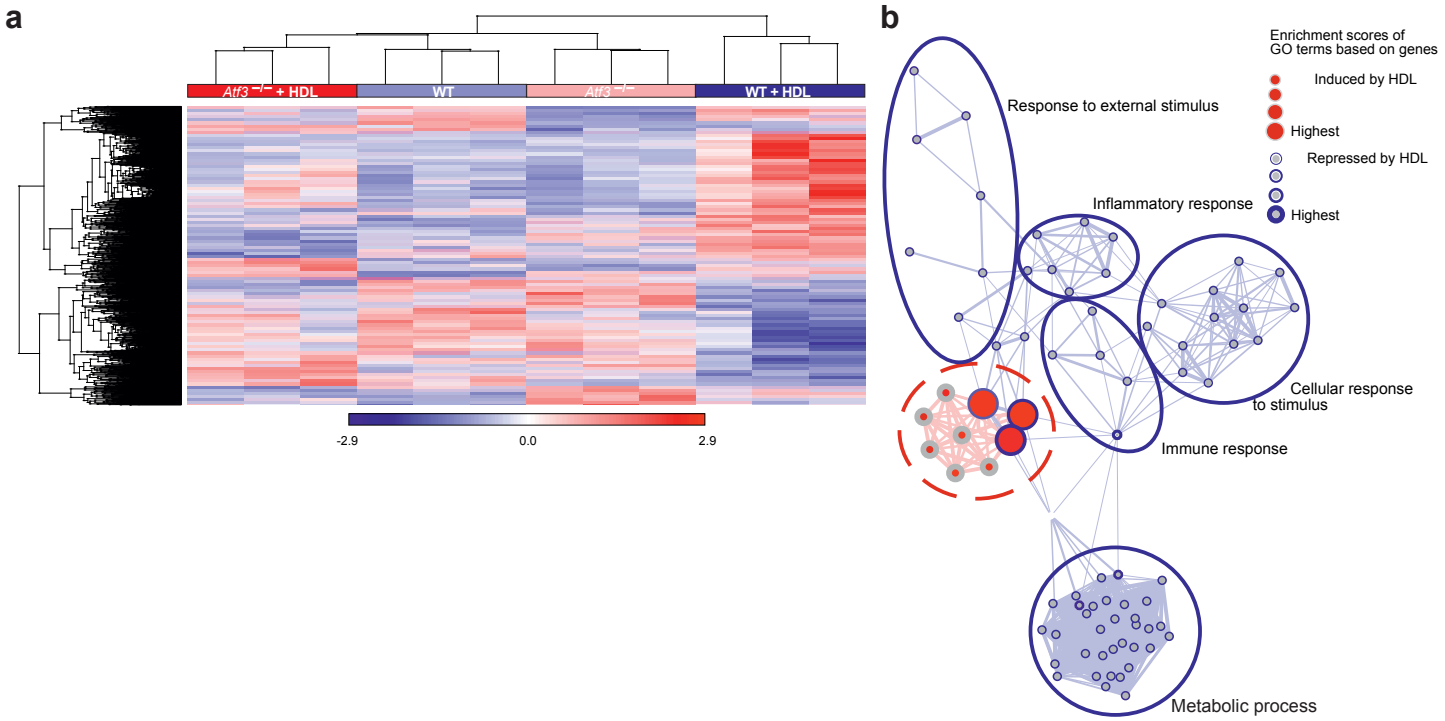

Supplementary Figure 6 Transcriptome analysis of carotid injury model. Transcriptome data derived from RNA of carotid arteries of mice subjected to endothelial injury 3 h prior to HDL (20 ug/kg) or PBS i.v. injection. **a** Hierarchical clustering of the 2073 most variable genes within the dataset. **b**, Network visualisation of Gene ontology enrichment analysis (GOEA) based on transcripts regulated in macrophages *in vitro* and in carotid arteries *in vivo*. Enrichment scores of GO-terms based on genes upregulated or downregulated by HDL in vivo. **a**, **b**, At least three biological replicates per condition were generated and analysed.